PHYSICAL REVIEW D VOLUME 19, NUMBER 9 1 MAY 1979

Flavoring and cylinder renormalizations of the Pomeron

S. T. Jones
Department of Physics, The University of Alabama, University, Alabama 35486
(Received 20 December 1978)

Flavoring and cylinder effects are synthesized in the context of the dual topological expansion. One finds a modified picture of the Pomeron-f identity, where mixing among planar trajectories has a threshold energy. A model is proposed incorporating these effects and is shown to have desirable features. It is further proposed that flavoring may be *entirely* a nonplanar phenomenon. Phenomenology based on this model shows the Pomeron-f identity to be compatible with existing data on vector-meson production.

I. INTRODUCTION

In the framework of the dual topological unitarization program,[1] it has been proposed that the Pomeron and f Regge singularities are one and the same. In this scheme, the f at the planar level is degenerate with the ρ, A_2, and ω, with intercept around 0.5. In addition, another neutral trajectory with quark content $s\bar{s}$ is presumed to lie below the f and contain the f' and ϕ. The f undergoes two significant renormalizations which prompt us to identify it with the Pomeron. The first effect is the cylinder contribution,[2] a first-order correction to the planar pole. This contribution also mixes f and f'. The second effect has been termed flavoring,[3] and is a threshold effect stemming from the higher mass of the strange (and charmed) quarks and diquarks. These effects have heretofore been considered separately, although there has been speculation that they are related.[2,4] We present here an analysis of the combined effects, and show that the two are interrelated in a significant way. The resulting phenomenology differs from and improves upon previous analyses, as will be indicated. This synthesis may therefore solve the difficulties that the model of Ref. 2 has had phenomenologically. We go on to suggest that flavoring may be purely a cylinder effect, and discuss the consequences of this assumption.

We restrict ourselves for the moment to meson-meson scattering, where the topological expansion is well understood. Our results can be extended to meson-baryon and baryon-baryon systems to the extent that baryonium exchanges can be neglected. We also ignore flavoring by $B\bar{B}$ pairs. Our numerical results will thus relate to moderate energies only (say, $P_{\text{lab}} \lesssim 50$ GeV/c). Our findings are that trajectories which are ideally mixed give the full contribution to scattering amplitudes below the threshold energy for $K\bar{K}$ production. Above this threshold, flavoring with cylinder topology induces a mixing of these trajectories which can be described either via complex poles or via an expansion using the unflavored poles. Mixing between f and f' is thus an energy-dependent phenomenon. However, cylinder corrections involving nonstrange quarks have no such threshold, and we conclude that it is this effect which renormalizes the f to its "unflavored" intercept around 0.85. Such an intercept has been found to be quite successful in describing low-energy data.[3,5]

Because the concept of flavored and unflavored poles can lead to confusion, let us review at this point the way in which thresholds are treated in this and similar analyses. We know that there is a minimum energy below which strange-particle production cannot occur. Energy conservation alone assures us that the $K\bar{K}$ threshold is above $\pi\pi$ threshold. We will use $K\bar{K}$ pairs to represent strange-particle production in general. The effect is much more pronounced than mere energy conservation would predict, however, and observed thresholds are markedly higher than one might naively expect. The explanation lies in the underlying dynamics, generally presumed to be multiperipheral for the bulk of the cross section. Because multiperipheral dynamics greatly enhances low-momentum transfers (i.e., small t_i), and because $|t_{\text{min}}|$ increases with the mass of the produced particles at fixed energy, heavy-particle production is greatly disfavored at low energies. It thus turns out to be a good approximation to say that there exists a threshold for $K\bar{K}$ production around $P_{\text{lab}} \approx 10$ GeV/c, even though the kinematic threshold is much lower and a small amount of $K\bar{K}$ production does occur below 10 GeV/c.

Now consider a multiperipheral model for strange- and nonstrange-particle production. Let us assume a threshold s_{th} below which strange particles are not produced. We will neglect any thresholds for nonstrange (mostly π) production. We can write the absorptive part of the forward amplitude in terms of the multiparticle final states as follows, using unitarity:

$$A(s)=\sum_n A_n(s)$$

$$=\sum_n\left(A_n^{ns}(s)+\sum_m A_{nm}^s(s)\right). \quad (1)$$

$A_{nm}^s(s)$ is the amplitude for production of m $K\bar{K}$ pairs, along with n nonstrange particles. We are also interested in the J-plane structure of the forward amplitude, given with sufficient accuracy by the Mellin transform

$$A(J)=\int_{s_0}^{\infty} ds\, s^{-J}A(s). \quad (2)$$

The inverse of (2) is

$$A(s)=\int \frac{dJ}{2\pi i}\, s^J A(J). \quad (3)$$

Now if we sum the entire series in (1), we get the full amplitude, which corresponds to a J-plane structure of a leading real pole (or several poles, in general) accompanied by a series of complex-conjugate pairs of poles. The latter arise from the thresholds $\theta(s-s_{\rm th})$ in $A_{nm}^s(s)$. Let us for simplicity consider only a single-channel problem for the moment, with only a single real pole α in $A(J)$. Because α is generated by all contributions to $A(s)$, including all flavors, we call α the "flavored" pole. (If all nondiffractive thresholds are included, α is then the bare pole, appropriate as input to the Regge field theory.)

An alternative and very useful approach is to add the two parts of Eq. (1) separately, leading to

$$A(s)=A^{ns}(s)+A^{s}(s)$$

$$=A^{ns}(s)+\sum_m A_m^s(s). \quad (4)$$

Because every term $A_m^s(s)$ has a threshold of at least $s_{\rm th}$, $A^{ns}(s)$ is equal to the *full* amplitude for $s<s_{\rm th}$, and is a good first approximation to it for $s\gtrsim s_{\rm th}$. We denote this low-energy amplitude and its poles by using a caret. Thus $A^{ns}(s)\equiv\hat{A}(s)$. Now, since production of m $K\bar{K}$ pairs has a threshold on the order of $(s_{\rm th})^m$, the series in Eq. (4) truncates at any finite energy, and it is advantageous to write the amplitude at moderate energies as a series:

$$A(s)=\hat{A}(s)+\hat{A}_1^s(s)+\hat{A}_2^s(s)+\cdots. \quad (5)$$

This series converges rapidly, and provides much physical insight into the energy dependence of $A(s)$.

The leading pole in $\hat{A}(J)$ is denoted by $\hat{\alpha}$. In the one-channel case we are considering here, $\hat{\alpha}$ and its daughters are the only poles in $\hat{A}$. We will ignore daughter poles in this paper. $\hat{\alpha}$ is called the unflavored pole, and is a singularity of $\hat{A}$, but *not* of A. [Note that $\hat{A}_m^s(J)$ has a pole of order m $+1$ at $J=\hat{\alpha}$ as indicated by the caret.] Nevertheless, at low energies $A(s)\equiv\hat{A}(s)=\beta s^{\hat{\alpha}}$, so it must be that the combination of the real pole α and all its accompanying complex poles is equivalent to the unflavored pole $\hat{\alpha}$. This has been demonstrated explicitly by Dash *et al.*,[3] who have developed this approach and explored many of its phenomenological implications. In particular, it has been demonstrated that an unflavored pole $\hat{\alpha}$ with intercept $\hat{\alpha}(0)\cong 0.85$ can be generated self-consistently in a multiperipheral model, and that the corresponding amplitude $\hat{A}(s)$ gives an excellent description of low-energy data.[5] An important ingredient in this model is the existence of only a single leading vacuum pole—that is, the Pomeron and f are one and the same.

Let us now consider a three-quark model in the context of the dual topological expansion. At the planar level, below flavoring thresholds (i.e., below $s_{\rm th}$), we will have two leading poles, called by Chew and Rosenzweig α_0 and α_3. The former has quark content $u\bar{u}$ and $d\bar{d}$, and is fourfold degenerate. ($I=1$ and $I=0$ are degenerate, as are $C=\pm$.) The content of α_3 is $s\bar{s}$, and α_3 is doubly degenerate ($C=\pm$), with an intercept somewhat below $\alpha_0(0)$. If we now add in the quark diagrams with the topology of the cylinder, the degeneracies are partly broken, and we might also expect some mixing between α_0 and α_3. We will show, however, that this mixing does not occur below the $K\bar{K}$ threshold. In other words, below $K\bar{K}$ threshold, where $A=\hat{A}$, we can write

$$A=\hat{A}=\hat{A}_0+\hat{A}_3,$$

where the poles in $\hat{A}_0$ and $\hat{A}_3$ are $(\hat{\alpha}_f, \hat{\alpha}_\omega, \hat{\alpha}_\rho, \hat{\alpha}_{A_2})$ and $(\hat{\alpha}_{f'}, \hat{\alpha}_\phi)$, with quark contents ($u\bar{u}$ and $d\bar{d}$) and $s\bar{s}$, respectively. Thus, the unflavored amplitude, which equals the full amplitude below $s_{\rm th}$, contains *ideally mixed* poles. Above $s_{\rm th}$, we can either write the full amplitude in terms of its poles (real and complex) or as a series analogous to Eq. (5). The latter is far more illuminating. We will see that some of the cylinder contributions to $\hat{A}_m^s(s)$ do in fact mix $\hat{\alpha}_f$ and $\hat{\alpha}_{f'}$ (also $\hat{\omega}$ and $\hat{\phi}$). Thus the fully flavored poles are mixtures of all three quarks, and can be identified with the f, f', ω, and ϕ. But at moderate energies, where the thresholds are important, the energy dependence is neither that of $\hat{\alpha}$ nor that of the flavored poles α_f, α_ω, etc. One must either use flavored plus complex poles, or unflavored poles plus the expansion of Eq. (5). It is in this sense that we say the mixing is energy dependent.

In the following section, we use quark diagrams to demonstrate the general mechanisms at work here. In Sec. III we formulate a simple model incorporating these ideas and investigate some of

its properties. Section IV is devoted to a preliminary investigation of the phenomenological aspects of the model, including some actual fits to total and partial cross sections. We discuss in the concluding section the successes and failures of the particular model and suggested improvements.

II. FLAVORING AND THE CYLINDER

We begin our analysis by considering the quark diagrams of Fig. 1. We assume a multiperipheral mechanism for generating the various trajectories through unitarity. Figure 1(a) shows a typical planar diagram with no strange or heavier quarks. Such diagrams generate the unrenormalized and degenerate f, ρ, ω, A_2 trajectories which we call collectively $\alpha_0(t)$ $[\alpha_0(0) \approx 0.5]$. Figure 1(b) shows the corresponding diagram for generating the f' and ϕ, which are ideally mixed and degenerate at the planar level. (The use of the terms f, f', ω, etc. here is potentially misleading, since α_0 and α_3 are not poles of the full amplitude, and the full poles are not planar nor ideally mixed. Since ideal mixing works much better for $t>0$, there *is* some sense in which we can label the trajectories this way. For the moment, we do so for bookkeeping as we examine how the physical trajectories evolve from the planar ones.) One consequence of the breaking of SU(3) is that the planar $s\bar{s}$ trajectory, which we call α_3 following Chew and Rosenzweig,[2] is lower than α_0, with $\alpha_3(0) \approx 0.1$–0.2.

Figure 1(c) is again a planar diagram, but now we include strange-quark loops. The intermediate state now contains strange particles, if we assume the strange-quark loop cannot be contracted to the topologically equivalent graph 1(a). The latter possibility is considered at the end of the next section. Since strange particles are heavier than *non*-strange particles ($m_K > m_\pi$, $m_{K^*} > m_\rho$) and must be produced in pairs, a threshold energy must be reached before strange particles can contribute to the unitarity sum. Thereafter this new component will renormalize the unflavored trajectory, as discussed in Sec. I. This process is called flavoring. The $K\bar{K}$ threshold is not high, say 10 GeV/c, but the effect is important in describing the energy dependence of cross sections.

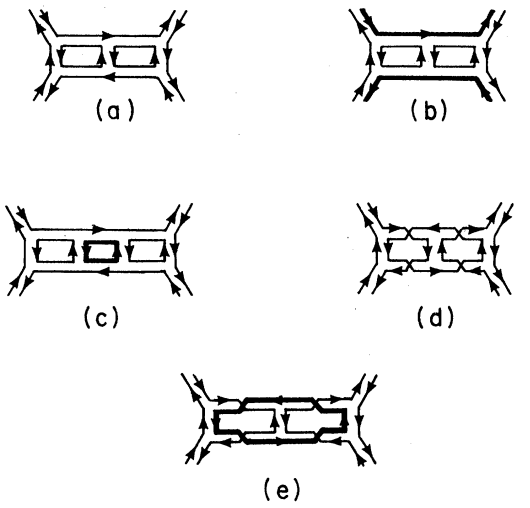

FIG. 1. Quark diagrams representing various contributions to the generation of Regge singularities. Bold lines indicate strange quarks. The t channel runs left to right.

Figures 1(d) and 1(e) show examples of the simplest nonplanar effects, referred to as cylinder diagrams. We observe that cylinder loops involving strange quarks must also involve strange-particle production, and thus observe a threshold energy. Note that we cannot contract the strange-quark loops into ordinary mesons here as suggested for Fig. 1(c). Nonstrange cylinder loops have a substantially lower threshold (usually neglected in model calculations), and contribute at low energies.

Of the diagrams in Fig. 1, only 1(e) generates a singularity which mixes $(u\bar{u}+d\bar{d})$ with $s\bar{s}$ (i.e., which mixes α_0 and α_3). We can conclude from this the following:

(a) Cylinder corrections renormalize α_0 at low energies but do not mix α_0 and α_3;

(b) Flavoring corrections (planar and nonplanar) renormalize both α_0 and α_3 only above a certain threshold energy;

(c) Mixing between α_0 and α_3, from cylinder corrections, occurs only above the $K\bar{K}$ threshold energy.

It is thus natural to assume that the unflavored Pomeron, $\hat{\alpha}_f$ $[\hat{\alpha}_f(0) \approx 0.85]$, is generated by all nonstrange contributions, both planar and nonplanar. This unflavored Pomeron is ideally mixed, as no mixing with α_3 has occurred.

An important special case occurs for $K\pi$ (KN) scattering. Figure 2(a) shows a single-twist diagram which will mix α_3 and α_0 and yet has the same threshold as the planar diagram, Fig. 2(b). This mixing will not renormalize the pole intercepts, but will affect the couplings.

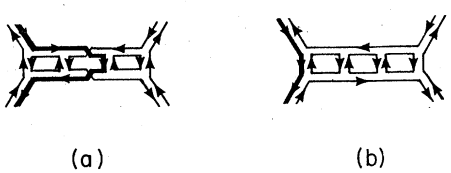

FIG. 2. Nonplanar (a) and planar (b) contributions to $K\pi$ scattering with the same threshold energy.

III. A MODIFIED CHEW-ROSENZWEIG MODEL

We can now reformulate the model of Chew and Rosenzweig[2] to incorporate both flavoring and cylinder renormalizations in one kernel. SU(3) breaking will now be explicit in the kernel, in contrast to the supposition of Ref. 2. We include the terms diagramed in Fig. 3, which yield the combined mixing and flavoring matrix for $I=0$. If we make a simple exponential parametrization for the threshold factors, we find a kernel for positive charge conjugation:

$$K(J)=\begin{pmatrix} 2kg^2+G^2e^{-2bJ} & \sqrt{2}\,kGge^{-bJ} \\ \sqrt{2}\,kGge^{-bJ} & G^2e^{-2bJ}(1+k) \end{pmatrix}. \tag{6}$$

Here k is the cylinder strength (relative to planar), g and G are the planar nonstrange- and strange-meson couplings, respectively, and b is the rapidity threshold required for production of a single strange meson. That the diagonal terms in G^2 have the twice this threshold (i.e., $2b$) means our strange particles are assumed to be produced in uncorrelated pairs. An alternative formulation will be considered below. The two channels of this matrix represent the ideally mixed $I=0$ states $(u\bar{u}+d\bar{d})/\sqrt{2}$, $s\bar{s}$, corresponding to α_0 and α_3, respectively. The $I=1$ kernel is just G^2e^{-2bJ}. The planar propagator matrix is

$$P=\begin{pmatrix} (J-\alpha_0)^{-1} & 0 \\ 0 & (J-\alpha_3)^{-1} \end{pmatrix} \tag{7}$$

and the amplitude is given by

$$A(J)=\sum_N \bar{V}(J)P(KP)^N V(J) \tag{8a}$$

$$=\bar{V}(J)P(1-KP)^{-1}V(J). \tag{8b}$$

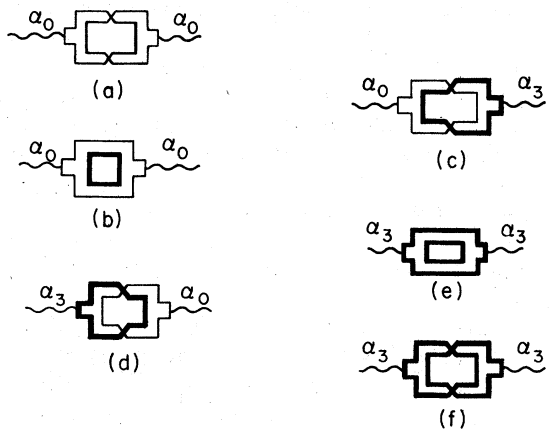

FIG. 3. Contributions which renormalize the trajectories α_0 and α_3. Strange quarks are represented by bold lines. The diagrams are arranged in the order that they appear in the kernel K [Eq. (6)].

$V(J)$ is the coupling to external particles, and is shown to explicitly depend on J. This dependence must be included for consistency, since we may have K production at the end of the multiperipheral ladder, as in Fig. 1(c). For $C=-$, the amplitude is obtained by replacing k by $(-k)$.

If we ignore flavoring, by setting $G=0$, we find poles as solutions of

$$(J-\alpha_0-2g^2k)(J-\alpha_3)=0. \tag{9}$$

We see that α_0 is renormalized by the cylinder to

$$\hat{\alpha}_f=\alpha_0+2g^2k\approx 0.85 \quad (\text{at } t=0). \tag{10}$$

α_3 is unchanged (so $\hat{\alpha}_{f'}=\alpha_3$). The negative-charge-conjugation ($C=-$) poles are

$$\hat{\alpha}_\omega=\alpha_0-2g^2|k|, \tag{11}$$

$$\hat{\alpha}_\phi=\alpha_3. \tag{12}$$

If we include the effects of flavoring, we find two leading real poles and a series of complex poles for each value of C, as in one-channel models of threshold effects. Phenomenological studies[3] indicate that $K\bar{K}$ flavoring ought to raise $\hat{\alpha}_f$ to $\alpha_f \approx 1.0$. We can accomplish this with a reasonable set of parameters. For example, if we let $b=0.7$, $k=1$, $\alpha_3=0.2$, $\alpha_0=0.5$, we find α_f (flavored) $=1.0$, $\alpha_\omega=0.53$, and an asymptotic (i.e., $P\approx 50$-GeV/c) mixing angle of $\theta_+\approx 17°$. θ_+ is defined such that

$$|f\rangle=\cos\theta_+|0\rangle+\sin\theta_+|3\rangle. \tag{13}$$

The fact that these numbers are reasonable is encouraging.

One problem we face with the present model is that the $J=1$ trajectories, though unaffected by the cylinder, will be flavored by the planar diagrams such that $\hat{\alpha}_\rho=0.5$, $\alpha_\rho\cong 0.65$, with the above parameters. Such threshold behavior is not observed: ρ-exchange cross sections are very well fitted by a single real pole near $\frac{1}{2}$.[6] We therefore wish to consider the possibility[7] that the *planar* flavoring contributions [Figs. 3(b) and 3(e)] do *not* have a significant threshold. For example, a planar $K\bar{K}$ pair may be bound or resonate. The pair is dual to ordinary mesons, and it may be improper to consider the $(u\bar{s})(s\bar{u})$ states in Fig. 3(b) to be literal K and $\bar{K}$ mesons. Even if not resonant, the pair is correlated and may very well have a low invariant mass ($\sim 2m_K$). In either case, we might expect this planar $K\bar{K}$ pair to exhibit itself as a relatively low mass unit, so that it is probable that the threshold factors for Figs. 3(b) and 3(e) are less than shown in Eq. (6). In contrast, the K's produced via a twist must be uncorrelated, with strange-particle (or ϕ) exchanges between them, and here the full threshold factor is appropriate ($m_{K\bar{K}} \gg 2m_K$). If these considerations are valid, we can

modify the kernel of Eq. (6) by dropping the threshold factors for Fig. 3(b), 3(e) and including *all* planar contributions in α_0 and α_3. The physical case may be intermediate between these extremes. The kernel is then

$$K^{\pm}(J)=\pm\begin{pmatrix} 2k & (2Kk)^{1/2}e^{-bJ} \\ (2Kk)^{1/2}e^{-bJ} & Ke^{-2bJ}\end{pmatrix}, \quad (14)$$

where we have absorbed g and G into k and K, respectively.

When we apply these considerations to our model, we find some interesting consequences which are attractive phenomenologically. Specifically, the unflavored $\omega(\hat{\alpha}_\omega)$ is now shifted down much less, and the mixing angle θ_+ is more realistic. For example, with $\alpha_3=0.2$, $\alpha_0=0.6$, and $b=1$, we find $\hat{\alpha}_f=0.85$, $\hat{\alpha}_\omega=0.35$. The flavored parameters are then $\theta_+=28.5°$, $\theta_-=-21.8°$, $\alpha_\omega=0.52$, $\alpha_{f'}=0.48$, and $\alpha_f=1.0$. The ϕ becomes entirely complex in this approach. The $I=1$ trajectories (ρ, A_2) are fixed at 0.6 in this version, and undergo no flavoring.

The fact that realistic numbers are obtained with this simple model is encouraging, even without detailed phenomenology. Before approaching the available data, however, we should point out some of the shortcomings of our present formulation of this model. Most important is our omission of interference diagrams, those with twists on the produced particles. As shown by Eylon and others,[8] an SU(3)-symmetric model cannot generate an ω at all if it neglects these terms. We have done so here primarily so that we can have a tractable model, without a large number of channels. The sensitivity of the ω and ϕ to details of the model warns us that this sector (i.e., $C=-$) may not be well treated in our model. We will see that this is in fact the case. Other obvious omissions are such things as cuts and associated production, found to be small but noticeable effects in earlier work; and our treatment of thresholds, via an exponential in J, is of course the simplest possible. Judging from other fits using similar models, we should not expect these latter effects to prevent us from achieving a reasonable description of data, and thus testing the basic content of the model.

In order to compare this model with experiment, we will have to make some specific assumptions concerning t dependence and baryon couplings. This will be done in the next section, but let us first consider some general features of this approach which lead us to believe it will improve upon earlier models. In particular, it has been shown that the model of Chew and Rosenzweig, while successful in describing total cross sections, fails to adequately fit vector-meson production processes ($PN\to VN$). We can demonstrate qualitatively why we believe the situation will be somewhat improved with the present version, and will show in the next section that a decent fit to $PN\to VN$ can be realized with a specific realization of our model. The remarks in the following paragraphs refer to both versions of the present model, unless otherwise noted.

First, consider the energy dependence of the total cross sections. Since $\hat{\alpha}_{f'}$ does not couple to $\pi\pi$ or $N\bar{N}$, we will have no contributions from it to $\sigma(\pi N)$ or $\sigma(NN)$ below $K\bar{K}$ threshold. Above this threshold, its contribution can almost certainly be neglected relative to that of $\hat{\alpha}_f$, and we are left with a description of πN and NN scattering in terms of nonstrange poles. In particular, the vacuum-exchange part of $\sigma(\pi N)$ and $\sigma(NN)$ will be described by the bare Pomeron plus flavoring corrections, very much as in Ref. 3. On the other hand, $\hat{\alpha}_{f'}$ *will* contribute to $\sigma(KN)$, through diagrams of the type of Fig. 2(a). Since this term is proportional to $(s^{\hat{\alpha}_f}-s^{\hat{\alpha}_{f'}})$, the $\hat{f}'$ contribution is negative and will lead to a flatter $\sigma(KN)$, as observed. In Ref. 3, this flattening was effected by eikonal cuts, which will not be needed here. The higher-energy behavior of $\sigma(KN)$ will be essentially that of α_f, as in Ref. 3. Thus, we expect the vacuum contribution to $\sigma(\pi N)$, $\sigma(NN)$, and $\sigma(KN)$ to behave much as they did in earlier fits. The relative normalizations will be free, but once fixed will determine the $PN\to VN$ couplings.

The $C=-$ contributions to the cross section can be compared to appropriate combinations of KN cross sections. These tend to behave roughly as $s^{-1/2}$, with little evidence of flavoring. We are led to conclude, then, that the second version of our model will be more successful, as in this instance the ω does not undergo very much flavoring ($\hat{\alpha}_\omega=0.35$, $\alpha_\omega=0.52$). However, we must keep in mind that the $C=-$ sector is not well treated when we neglected interference diagrams.

Turning now to the processes $PN\to VN$, we can use $\pi N\to\rho N$ to fix the ω parameters. Presuming this is successful (again, with $\alpha_\omega\sim 0.5$, this description is known to work), we are left with the problem of fitting the K^* data. The primary difficulties revealed by previous analyses[9,10] are the overall normalization (too large), and the energy dependence (σ falls too slowly). We can expect in the present model that the cross section will eventually be dominated by the Pomeron, which will not decouple since it will not be pure singlet (according to total cross sections). As for the overall normalization, the analysis of Tan *et al.*[10] found that the best fit was obtained if there was no mixing of α_0 and α_3 in the $C=-$ sector. Since we have no mixing here below $K\bar{K}$ threshold, we can

hope that our normalization will likewise be satisfactory. While we also have no mixing in the positive C sector (in contrast to Ref. 10), this will be partially offset by the contribution of Fig. 2(a). More specifically, while the planar f contributions will be enhanced over f' below $K\bar{K}$ threshold, the contribution of Fig. 2(a) goes like $(-s^{\hat{\alpha}_f}+s^{\hat{\alpha}_{f'}})$, partially canceling this enhancement. These qualitative features appear to be just what are required to describe K^* data, but because this model is more complex than that without thresholds, it is quite impossible to say for sure that a reasonable description can be obtained without doing a detailed phenomenology. Our attempt at this is described in the next section.

IV. A PHENOMENOLOGICAL ANALYSIS

In light of the considerations of the previous section, we choose the second formulation of our model for data fitting. Thus, all flavoring is in the cylinder. The amplitude is obtained from Eqs. (3), (8a), (7), and (14). In order to fit total cross sections, we need only choose our particle couplings $V(J)$. We make the simple choices ($C=\pm$)

$$V_{\pi\pi}=g\begin{pmatrix}1\\0\end{pmatrix},$$
$$V_{KK}=g\begin{pmatrix}1/2\\1/\sqrt{2}\end{pmatrix},$$
$$V_{NN}^{C}=\beta^{C}\begin{pmatrix}e^{-BJ}\\0\end{pmatrix} \tag{15}$$
$$V_{\pi\rho}=\bar{g}\begin{pmatrix}1\\0\end{pmatrix},$$
$$V_{KK^*}=\bar{g}\begin{pmatrix}1/2\\-1/\sqrt{2}\end{pmatrix}.$$

The meson vertices are fixed by SU(3), with g and $\bar{g}$ representing the PP and PV couplings, respectively. We couple nucleons only to nonstrange trajectories, and allow for different couplings for $C=\pm$. We include a threshold term e^{-BJ} for the nucleon. This is the only way to allow for different energy dependences of $\sigma(\pi N)$ and $\sigma(NN)$. The parameter s_0 in Eq. (2) is fixed at 1 GeV^2. Explicit formulas are listed in the Appendix.

We first fit the vacuum-exchange cross sections[11]

$$\sigma_0(NN)=[\sigma(\bar{p}p)+\sigma(pp)]/2,$$
$$\sigma_0(\pi N)=[\sigma(\pi^+p)+\sigma(\pi^-p)]/2, \tag{16}$$

and

$$\sigma_0(KN)=[\sigma(K^+p)+\sigma(K^-p)+\sigma(K^+n)+\sigma(K^-n)]/4.$$

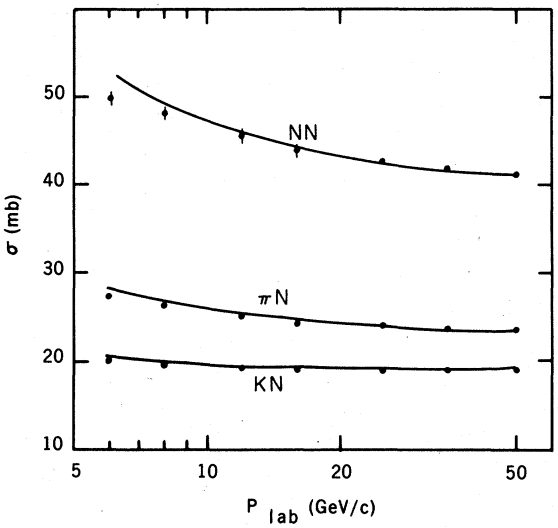

FIG. 4. Vacuum-exchange parts of the total cross sections NN, πN, and KN.

The free parameters are B, k, g, β^+, and b. k is fixed by the planar flavoring to be 0.125 ($\hat{\alpha}_f-\alpha_0=2k$). Our normalization is

$$\sigma(s)=\frac{1}{q\sqrt{s}}\,\mathrm{Im}A(s,0). \tag{17}$$

We fit representative data by expanding $A(s)$ as in Eq. (4), with the results as shown in Fig. 4. The parameters are listed in Table I. We see that the cross-section fits, though perhaps not as good as Ref. 3, are quite satisfactory. We have simultaneously fitted the K^- multiplicity in σ_{NN} to check that the energy dependence of σ is correlated to the flavoring due to $K\bar{K}$ production. The resultant multiplicity is shown in Fig. 5.

We next turn to the negative-C, $I=0$ cross section. We wish to fit

$$\sigma^-(KN)\equiv[\sigma(K^-p)-\sigma(K^+p)+\sigma(K^-n)-\sigma(K^+n)]/4. \tag{18}$$

Unfortunately, when we look at the theoretical cross section, we find that the "ω problem" has materialized here in the form of an unrealistic ϕ pole. Specifically, the $\hat{\phi}$ becomes complex with an intercept whose real part is around 0.4. This causes a totally unrealistic $C=-$ amplitude. Our approach to this problem is to assume that inclu-

TABLE I. Fitted parameters.

$g=$ 5.16	$K(0)=2.44$
$\bar{g}=$ 0.89	$k(0)=0.125$
$\beta^+=11.2$	$B=0.22$
$\beta^-=10.85$	$b=0.98$
$\gamma^+=$ 1.05	$\gamma^-=3.0$

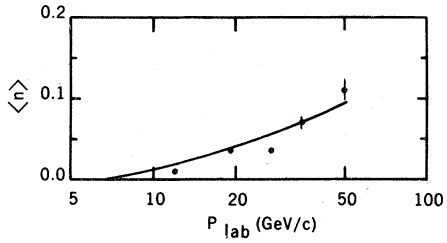

FIG. 5. K^- multiplicity in NN scattering, plotted versus P_{lab}.

sion of interference diagrams will fix the $C=-$ sector without seriously affecting the rest, as was indicated in Eylon's analysis.[8] In order to proceed with the analysis, we keep the $\hat{\omega}$, which is reasonable, and drop the $\hat{\phi}$, which is unrealistic in this model. This is the only correction we will apply to the model. Having done this, we have the resulting fit shown in Fig. 6. The only free parameter is β^-, which is given the value listed in Table I.

The effects of flavoring are evident in Figs. 4 through 6. Without flavoring, we would have simple power-law dependence of σ on s. In the fits of Ref. 10 the departure from power-law behavior was due to the f' contribution, absent here. The fact that the effective ω intercept is never far from 0.5 allows us to achieve an acceptable fit to $\sigma_\omega(KN)$ over a wide range of energies. The flattening of $\sigma_0(KN)$ is evident. In general, the quantitative features of the total cross sections are well fitted. We could look at the nonvacuum contributions to $\sigma(\pi N)$ and $\sigma(NN)$, but this would involve not only the ω but also the ρ trajectory. Since we are not primarily interested in the ρ, we will not pursue this analysis here. We note that our α_ρ is reasonable and does not get flavored, and expect that with a new free parameter β^ρ we should have no trouble fitting these additional data. We move now to the more challenging problem of vector-meson cross sections.

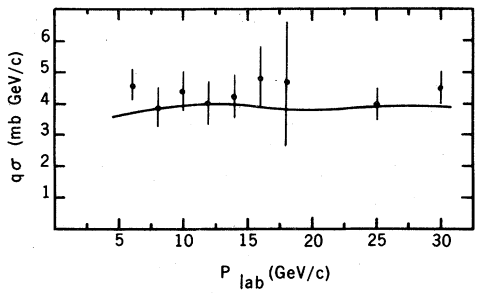

FIG. 6. The ω contribution to the KN total cross section. We plot $q\sigma$ versus laboratory momentum, where q is the center-of-mass momentum. The flatness of $q\sigma$ indicates that the amplitude is proportional to $\sqrt{s}$.

In order to study vector-meson cross sections, we must make some assumptions about the t dependence of our model. We choose b and B, our threshold parameters, to be independent of t. The parameters β^C and $\bar{g}$ will be given exponential t dependence. K and k must also vary with t, in a way which is qualitatively understood on general grounds.[2] We expect k and K to increase as $t \to -\infty$, so that the poles approach exact SU(3) symmetry. For $t>0$, according to the hypothesis of asymptotic planarity, k and $K \to 0$. The exact form of this t dependence is not known, so we choose it to be linear in the region of interest to us. We fix the slopes by demanding that the flavored trajectories be reasonable. Previous work has shown that the unflavored Pomeron ($\hat{\alpha}_f$) has a slope around 0.5, while the flavored Pomeron has a somewhat smaller slope. Flavoring becomes more significant for $t<0$ because the t_{min} effects are not as important. Furthermore, we expect the flavored ω and f' to have slopes around 1. This can be accomplished if we choose

$$K(t)=K_0-1.5t,\qquad k(t)=k_0-0.2t. \tag{19}$$

[Recall that $K(t)$ always appears in combination with e^{-bJ}, so $K \gg k$.] The resultant leading trajectories are shown in Fig. 7. They are approximately linear out to $t=-1$ (GeV/c)^2, and for our numerical work we use the approximations

$$\alpha_f(t)=1.02+0.23t,\qquad \alpha_{f'}(t)=0.49+0.89t,\qquad \alpha_\omega(t)=0.53+0.96t. \tag{20}$$

As input, we use

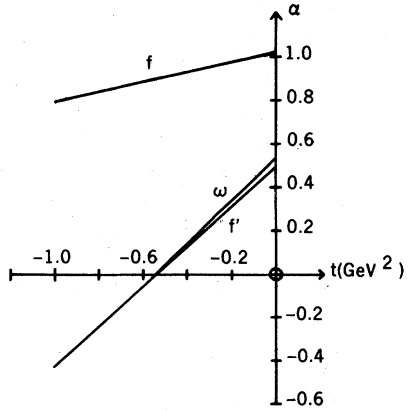

FIG. 7. Leading (real) trajectories generated by the model.

TABLE II. Poles in the *full* amplitude are at the values below. Complex poles occur in conjugate pairs; only the leading pairs are listed.

	Re $\alpha(t)$	Im $\alpha(t)$
$C=+$		
(f)	$1.02+0.23t$	...
(f')	$0.49+0.89t$	...
	$0.01-0.24t$	$2.31-0.16t$
	$-0.42-0.27t$	$5.53-0.08t$
$C=-$		
(ω)	$0.53+0.96t$	...
	$-0.25-0.24t$	$3.98-0.2t$
	$-0.55-0.27t$	$7.18-0.12t$
(ϕ) [a]	$0.43+0.18t$	$1.04-0.26t$

[a]Not used in fits.

$$\hat{\alpha}_f(t)=0.85+0.6t,$$
$$\hat{\alpha}_\omega(t)=0.35+1.4t, \tag{21}$$
$$\alpha_3(t)=0.2+t=\hat{\alpha}_{f'}(t),$$

and

$$\alpha_0(t)=0.6+t.$$

Note that $\hat{\alpha}_{f,\omega}(t)=\alpha_0(t)\pm 2k(t)$.

We cannot use Eq. (4) for this part of the analysis, since the *real* parts of the amplitude do not observe the thresholds (except in an approximate way, as shown in Ref. 3). We must instead use the full amplitude, which we represent in terms of its poles. We take the first two complex conjugate pairs of poles in addition to the real poles listed in Eq. (20) above. The expressions for the complex poles are listed in Table II. Note their negative slopes, reflecting the increased flavoring as $t\to-\infty$.

We then write our amplitude as

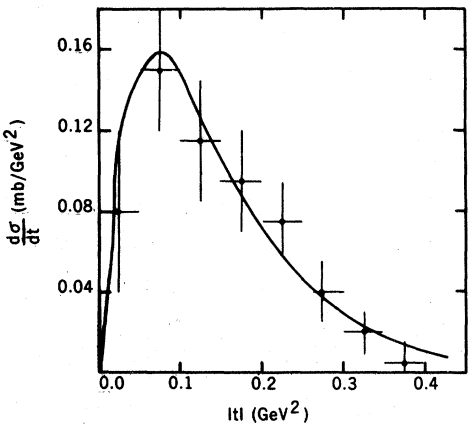

FIG. 8. The ω contribution to $(d\sigma/dt)(\pi N\to\rho N)$.

$$A(s,t)=\int\frac{dJ}{2\pi i}\,\xi(J)e^{iJ\Upsilon}A(J,t)$$
$$=\sum_i\xi(\alpha_i)e^{\alpha}i^{\Upsilon}N(\alpha_i)/D'(\alpha_i), \tag{22}$$

where N/D' is the residue of the ith Regge pole, with

$$D'(\alpha_i)=\left.\frac{\partial D}{\partial J}\right|_{J=\alpha_i(t)}. \tag{23}$$

$\xi(\alpha)$ is the signature factor. The functions N and D' are given in the appendix, along with a more detailed description of the parametrization.

We are now ready to compare these amplitudes to the vector-meson data. We have three new parameters: $\bar{g}$, γ^+, and γ^- ($\gamma^\pm$ are the exponential slopes—see Appendix). We fix $\bar{g}$ and γ^- by fitting the ω contribution to $(d\sigma/dt)(\pi N\to\rho N)$.[12] The resulting fit is shown in Fig. 8 and the parameters are as given in Table I. There remains only the parameter γ^+ to vary in order to achieve a fit to the K^* data.[13] One finds a fairly good fit with a reasonable value of γ^+, as seen in Figs. 9–12. We have fitted differential cross sections for both K^+ and K^- processes at several energies. We show representative examples in Figs. 9 and 10, and the integrated cross sections in Figs. 11 and 12. We find that our normalization is not bad, although the model is now too *small* at lower energies. (It was too *large* in Ref. 10.) The energy dependence is not bad, but it is clear that the Pomeron component is becoming increasingly important at higher energies. If the trend of the data does not shift to a less rapid fall at higher energies, the model and data will be in significant disagreement by around $P_{\rm lab}=100$ GeV/c. This prediction would seem to hold for any form of the model in which the Pomeron is identified with the f and must play a significant role in K^* processes.

If we relax the restriction that the f and f' residues have the same t dependence, we get a slightly improved fit with $\gamma^f=2.4$, $\gamma^{f'}=1.1$. This larger value of the Pomeron diffractive slope is somewhat more conventional. We also should point out that we have ignored unnatural-parity-exchange contributions to this process, which are known to be present in the data at about the 10% level. This should have no appreciable effect on our results.

V. SUMMARY AND CONCLUSIONS

We have formulated in general terms the relation between flavoring and cylinder effects, and found mixing of trajectories to be a flavoring effect. In other words, trajectories which are ideally mixed at the planar level will exhibit mixing only above the threshold energy for strange-particle produc-

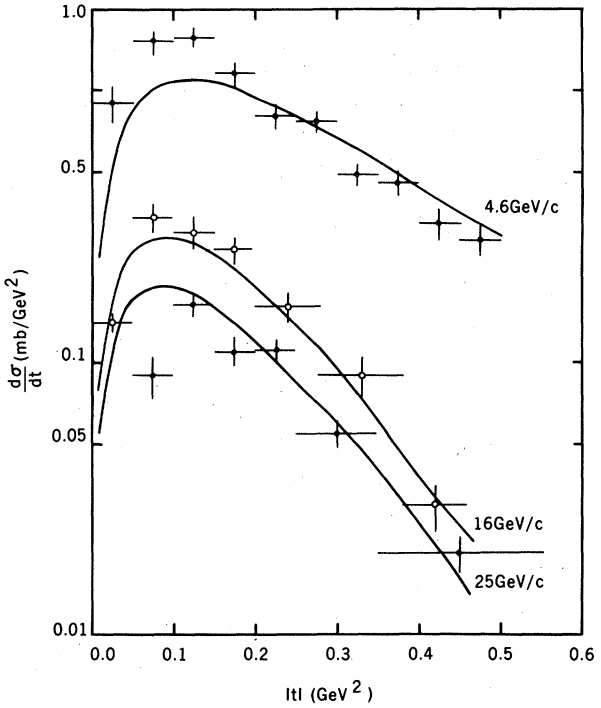

FIG. 9. $(d\sigma/dt)(K^-p \to K^{*-}p)$ at representative incident momenta.

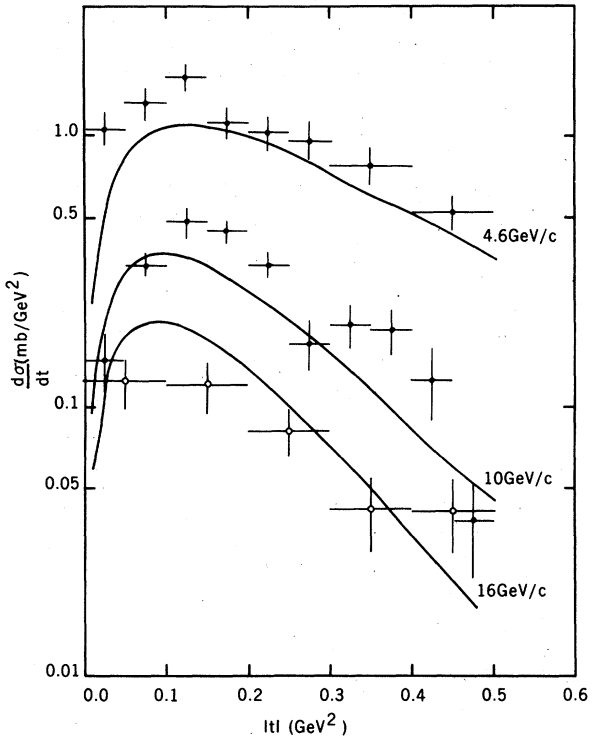

FIG. 10. $(d\sigma/dt)(K^+p \to K^{*+}p)$ at representative incident momenta.

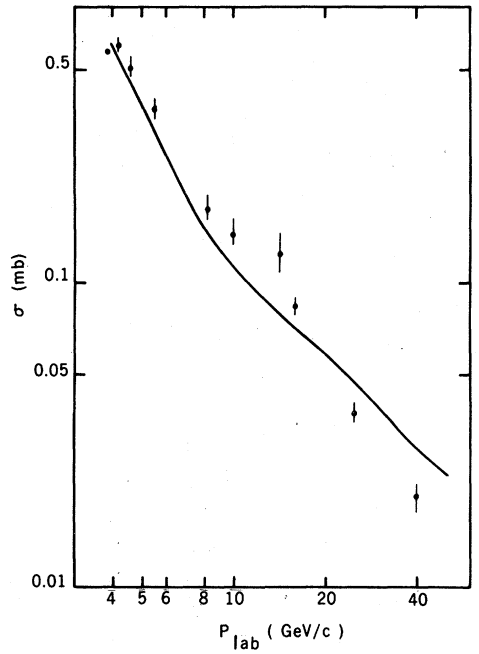

FIG. 11. Integrated cross section for $K^-p \to K^{*-}p$ plotted versus incident momentum.

tion. A specific model was constructed along the lines of that of Chew and Rosenzweig, and found to have generally desirable features. If we assumed that flavoring effects were to be found *only* in cylinder topologies, our model became more fav-

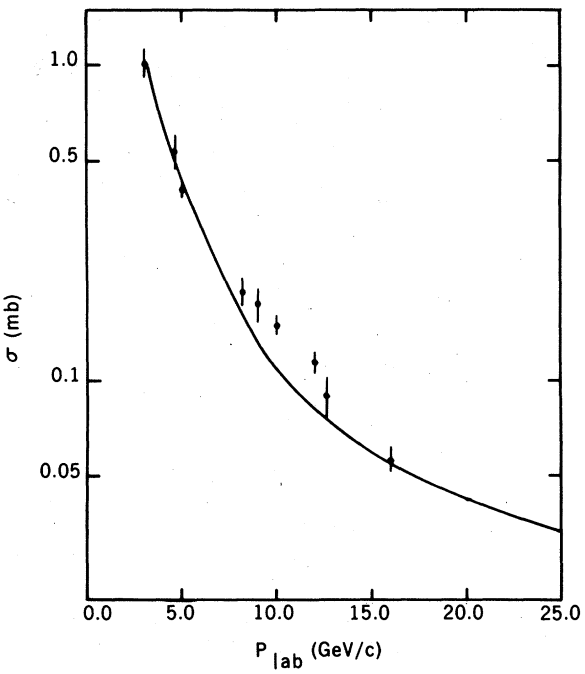

FIG. 12. $\sigma(K^+p \to K^{*+}p)$ versus incident momentum.

orable phenomenologically, and in fact was shown to be in reasonable agreement with experiment, except for some difficulty with the ω-ϕ sector. To the extent that our treatment of the "ω problem" was valid, we can conclude that the model and experiment are compatible for total cross sections and for vector-meson production up to at least 40 GeV/c, but that measurements of K^* production at only moderately higher energies will be crucial in testing the model. Incorporating flavoring into the Chew-Rosenzweig model has proved to have desirable effects on the overall phenomenology.

The model which proved best from a phenomenological standpoint was that which had only nonplanar flavoring. It then followed that the ρ and A_2 underwent no flavoring, as observed for the p.[6] The ω was shifted only slightly by flavoring, again in accord with total-cross-section measurements. We can make further observations. For one, it follows from Fig. 1(e) that a K and $\bar{K}$ will not in general be produced adjacent to one another in cylinder diagrams. It was shown in Ref. 14 that this is in fact required if inclusive data are to be explained by the same mechanism which is responsible for rising total cross sections. We also observe that only Okubo-Zweig-Iizuka- (OZI) rule-forbidden $K\bar{K}$ production will occur. This can be tested by comparing $\phi K\bar{K}$ production (allowed) to $(K\bar{K})(K\bar{K})$. The latter is at least partly cylinder and OZI-rule forbidden. Unfortunately, phase space for these processes is limited at current energies. It is known that OZI-rule-forbidden ϕ production (no accompanying $K\bar{K}$) predominates over $\phi K\bar{K}$,[15] but this could be due to phase space.

We have ignored baryon-antibaryon production in this model, primarily because a topological expansion for baryons is not yet full established. There is every indication, however, that baryonium mixing will follow the same general pattern as strangeness mixing—i.e., there will be a threshold for the mixing, namely the baryon-antibaryon effective threshold (around $P_{\text{lab}} = 100$ GeV/c). We have examined this process in the context of the ordered S matrix of Chew *et al.*,[16] and do in fact find this threshold effect to be present, though in an altered form. The theory is not yet sufficiently developed to lead to quantitative analysis, however, and we do not pursue it here. We should note, however, that it is only the imaginary parts of amplitudes that have thresholds. It was found in Ref. 3 that real parts do behave as if they were roughly observing thresholds, by interpolating between the unflavored Re$\hat{A}$ and the flavored ReA. But there remains the possibility that new high-mass thresholds such as baryon-antibaryon production can affect the phenomenology of K^* production at moderate momenta such as $P_{\text{lab}} \sim 40$ GeV/c.

ACKNOWLEDGMENTS

The author wishes to thank Professor G. F. Chew for the hospitality of Lawrence Berkeley Laboratory, where most of this work was completed. Conversations with Professor Chew and with Y. Eylon are gratefully acknowledged. This work was supported in part by the United States Department of Energy, and in part by the National Science Foundation, under Grant No. PHY 77-05300.

APPENDIX

We list here the formulas used in our analysis. For the total cross sections, we have the following relation for the absorptive part of the forward amplitude:

$$A(s) = \int \frac{dJ}{2\pi i} e^{JY} A(J), \tag{A1}$$

$$A_{ab}(J) = V_a^T(J)\hat{P}(J)(1-\hat{K}\hat{P})^{-1}V_b(J), \tag{A2}$$

where

$$\hat{K} = C \begin{pmatrix} 0 & (2Kk)^{1/2}e^{-bJ} \\ (2Kk)^{1/2}e^{-bJ} & Ke^{-2bJ} \end{pmatrix}, \quad C = \pm \tag{A3}$$

$$\hat{P} = \begin{pmatrix} (J-\hat{\alpha})^{-1} & 0 \\ 0 & (J-\alpha_3)^{-1} \end{pmatrix}, \tag{A4}$$

where

$$\hat{\alpha} = \begin{cases} \hat{\alpha}_f, & C = + \\ \hat{\alpha}_\omega, & C = - \end{cases}. \tag{A5}$$

We expand $(1-\hat{K}\hat{P})^{-1}$ and evaluate the integrals to get the amplitudes

$$A_{NN} = \beta^2 \left\{ \exp[\hat{\alpha}_f(Y-2B)] + \theta(z)\frac{(2Kk)^{1/2}}{\Delta^2}[e^{z\alpha_3} + e^{z\hat{\alpha}}(z\Delta - 1)] \right\}, \tag{A6}$$

where $z = Y - 2(b+B)$, $\Delta = \hat{\alpha}_f - \alpha_3$, $Y = \ln(s/s_0)$.

$$A_{\pi N} = g\beta \left\{ e^{z_0\hat{\alpha}_f} + \theta(z_2)\frac{(2Kk)^{1/2}}{\Delta^2}[e^{z_2\alpha_3} + e^{z_2\hat{\alpha}_f}(z_2\Delta - 1)] \right\}, \tag{A7}$$

$$A_{KN} = \tfrac{1}{2} g\beta \left\{ e^{z_0 \hat{\alpha}_f} + \theta(z_1) \frac{(2Kk)^{1/2}}{\Delta} (e^{z_1 \hat{\alpha}_f} - e^{z_1 \alpha_3}) + \frac{2Kk}{\Delta^2} \theta(z_2)[e^{z_2 \alpha_3} + e^{z_2 \hat{\alpha}_f}(z_2\Delta - 1)] \right.$$
$$\left. + \frac{2K(Kk)^{1/2}}{\Delta^2} \theta(z_3) \left[e^{z_3 \hat{\alpha}_f} - e^{z_3 \alpha_3}(z_3\Delta + 1) + \left(\frac{2k}{K}\right)^{1/2} [e^{z_3 \hat{\alpha}_f}(z_3 - 2/\Delta) + e^{z_3 \alpha_3}(z_3 + 2/\Delta)] \right] \right\} , \quad \text{(A8)}$$

where $z_n = Y - B - nb$. We have kept all terms in the expansion (4) of the text up to and including one produced $K\bar{K}$ pair. Comparison with Fig. 6 shows that one $K\bar{K}$ pair is sufficient to account for the multiplicity up to the energies considered in this paper.

The total cross section is obtained from

$$\sigma(s) = \frac{0.389}{q\sqrt{s}} A(s) . \quad \text{(A9)}$$

The vector-meson production amplitudes are derived from

$$T(s,t) = \int \frac{dJ}{2\pi i} \xi(J) e^{JY} A(J,t) , \quad \text{(A10)}$$

with

$$\xi(J) = -(e^{-i\pi J} \pm 1)/\sin\pi J . \quad \text{(A11)}$$

K, k, $\hat{\alpha}$, and α_3 are given t dependence as described in the text. Then we write

$$A(J,t) = N(J,t)/D(J,t)$$

with (A12)

$$D(J,t) = (J - \alpha_3)(J - \hat{\alpha}) - C(J - \hat{\alpha})Ke^{-2bJ} - 2Kke^{-2bJ} .$$

$A(J,t)$ has poles where $D(J,t)$ vanishes. Near the pole, we write

$$D(J,t) \approx (J - \alpha) D'(\alpha) , \quad \text{(A13)}$$

where

$$D'(\alpha) = \frac{\partial D}{\partial J}\bigg|_{J=\alpha} . \quad \text{(A14)}$$

Then

$$T(s,t) = \sum_i \xi(\alpha_i) e^{\alpha_i Y} N(\alpha_i)/D'(\alpha_i) . \quad \text{(A15)}$$

The numerator functions are

$$N^{(\alpha)}_{\pi N \to \rho N} = \bar{g}\beta^- \sqrt{-t}\, e^{-B\alpha}(\alpha - \alpha_3 + Ke^{-2b\alpha}) e^{\gamma^- t} , \quad \text{(A16)}$$

$$N^{\pm(\alpha)}_{KN \to K^* N} = \bar{g}\beta^{\pm} \sqrt{-t}\, e^{-B\alpha} [\tfrac{1}{2}(\alpha - \alpha_3 \mp Ke^{-2b\alpha}) \mp (Kk)^{1/2} e^{-b\alpha}] e^{\gamma^{\pm} t} . \quad \text{(A17)}$$

Finally, we get the differential cross section from

$$\frac{d\sigma}{dt} = \frac{0.389}{q^2 s} |T|^2 . \quad \text{(A18)}$$

[1] G. F. Chew and C. Rosenzweig, Phys. Rep. 41C, 5 (1978).

[2] G. F. Chew and C. Rosenzweig, Phys. Rev. D 12, 3907 (1975); P. Stevens, G. F. Chew, and C. Rosenzweig, Nucl. Phys. B110, 355 (1976).

[3] J. Dash and S. T. Jones, Nucl. Phys. B120, 345 (1977); J. Dash, S. T. Jones, and E. Manesis, Phys. Rev. D 18, 303 (1978).

[4] J. Dash, Phys. Lett. 61B, 199 (1976).

[5] N. F. Bali and J. W. Dash, Phys. Lett. 51B, 99 (1974); Phys. Rev. D 10, 2102 (1974); J. Dash, *ibid.* D 9, 200 (1974).

[6] A. Garcia, C. A. Garcia Canal, and L. Masperi, Phys. Rev. D 17, 917 (1978).

[7] This possibility was suggested to the author by G. F. Chew.

[8] Y. Eylon, Nucl. Phys. B118, 119 (1977); C. Schmid and C. Sorensen, *ibid.* B96, 209 (1975).

[9] D. W. Duke, Phys. Lett. 71B, 347 (1977).

[10] C.-I Tan, D. Tow, and J. Tran Thanh Van, Phys. Lett. 74B, 115 (1978).

[11] Data for total cross sections are from W. Galbraith *et al.*, Phys. Rev. 138, B913 (1965); S. P. Denisov *et al.*, Phys. Lett. 36B, 415 (1971); 36B, 528 (1971); Nucl. Phys. B65, 1 (1973).

[12] A. P. Contogouris, J. Tran Thanh Van, and H. J. Lubatti, Phys. Rev. Lett. 19, 1352 (1967).

[13] Data from K. Barnham *et al.*, Nucl. Phys. B28, 171 (1971); C. Fu *et al.*, *ibid.* B28, 528 (1971); M. Anguilar-Benitez *et al.*, Phys. Rev. D 4, 2583 (1971); Yu. M. Antipov *et al.*, Nucl. Phys. B63, 202 (1973); V. Waluch *et al.*, Phys. Rev. D 8, 2837 (1973); P. Estabrooks *et al.*, *ibid.* 17, 658 (1978); D. Colley *et al.*, Nucl. Phys. B110, 333 (1976); H. G. J. M. Tiecke *et al.*, *ibid.* B39, 596 (1972); R. Engelmann *et al.*, Phys. Rev. D 5, 2162 (1972); E. Zevgolatakos *et al.*, Nucl. Phys. B55, 15 (1973); M. Deutschmann *et al.*, *ibid.* B36, 373 (1972); B81, 1 (1974); B. Chaurand *et al.*, Phys. Lett. 38B, 253 (1972); V. Gordon Lind *et al.*, Nucl. Phys. B14, 1 (1969); J. Berlinghieri *et al.*, *ibid.* B8, 333 (1969).

[14] S. T. Jones, Phys. Rev. D 18, 726 (1978).

[15] C. W. Akerlof *et al.*, Phys. Rev. Lett. 14, 861 (1977).

[16] G. F. Chew, J. Finkelstein, J. P. Sursock, and G. Weissmann, Nucl. Phys. B136, 493 (1978).